Journal of Coordination Chemistry

ISSN: 0095-8972 (Print) 1029-0389 (Online) Journal homepage: http://www.tandfonline.com/loi/gcoo20

Heteroleptic Pd(II) dithiocarbamates: synthesis, characterization, packing and in vitro anticancer activity against HeLa cell line

Shahan zeb Khan, Muhammad Kashif Amir, Muhammad Moazzam Naseer, Rashda Abbasi, Kehkashan Mazhar, Muhammad Nawaz Tahir, Iqra Zubair Awan & Zia-Ur-Rehman

To cite this article: Shahan zeb Khan, Muhammad Kashif Amir, Muhammad Moazzam Naseer, Rashda Abbasi, Kehkashan Mazhar, Muhammad Nawaz Tahir, Iqra Zubair Awan & Zia-Ur-Rehman (2015) Heteroleptic Pd(II) dithiocarbamates: synthesis, characterization, packing and in vitro anticancer activity against HeLa cell line, Journal of Coordination Chemistry, 68:14, 2539-2551, DOI: 10.1080/00958972.2015.1054817

To link to this article: http://dx.doi.org/10.1080/00958972.2015.1054817

Journal of Coordination Chemistry, 2015
Vol. 68, No. 14, 2539–2551, http://dx.doi.org/10.1080/00958972.2015.1054817

Heteroleptic Pd(II) dithiocarbamates: synthesis, characterization, packing and *in vitro* anticancer activity against HeLa cell line

SHAHAN ZEB KHAN†‡, MUHAMMAD KASHIF AMIR†, MUHAMMAD MOAZZAM NASEER†, RASHDA ABBASI§, KEHKASHAN MAZHAR§, MUHAMMAD NAWAZ TAHIR¶, IQRA ZUBAIR AWAN‖ and ZIA-UR-REHMAN*†

†Department of Chemistry, Quaid-i-Azam University, Islamabad, Pakistan
‡Department of Chemistry, University of Science & Technology, Bannu, Pakistan
§Institute of Biomedical and Genetic Engineering (IBGE), Islamabad, Pakistan
¶Department of Physics, University of Sargodha, Sargodha, Pakistan
‖Department of Chemistry, Lahore College for Women University, Lahore, Pakistan

(*Received 17 December 2014; accepted 2 May 2015*)

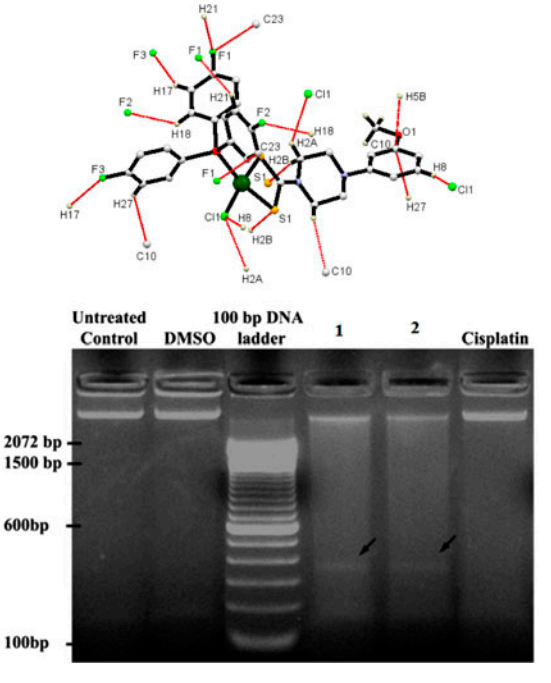

*Corresponding author. Email: zrehman@qau.edu.pk

The paper presents two new heteroleptic Pd(II) dithiocarbamates (**1** and **2**) and their outstanding anticancer properties.

Two new heteroleptic Pd(II) dithiocarbamates (**1** and **2**) have been synthesized by reaction of equimolar quantities of palladium(II) chloride, sodium 4-(3-methoxyphenyl)piperazine-1-carbodithioate, and appropriate substituted triphenylphosphines. The synthesized complexes have been characterized by their physical, spectral (IR, ^{1}H, ^{13}C, and ^{31}P NMR), and X-ray crystallographic data. Complexes **1** and **2** showed square-planar geometry both in solution and solid states. The crystal packing of both complexes revealed similar 3-D-supramolecular networks comprised of 1-D chains. However, the nature and strength of various non-covalent interactions of these networks were slightly different. The DNA interaction studies of the complexes have been carried out by UV–visible spectroscopy to evaluate their anticancer potential. The study suggested intercalative interaction with 2.402×10^4 and 2.713×10^3 M^{-1} binding constants, respectively. The complexes have also been evaluated for their anticancer activity against HeLa cell line. Both complexes showed higher activity with IC_{50} values much lower (22.176 and 26.166 μM for **1** and **2**, respectively) than the standard cisplatin (78.075 μM). Furthermore, the complexes induced stronger DNA fragmentation as investigated by DNA ladder assay for apoptosis. Our findings suggested that the anticancer action of these compounds stems from their interaction with DNA leading to DNA damage and apoptosis. The excellent activity of **1** and **2** deserves to be a focus for further research and *in vivo* studies.

Keywords: Pd(II) dithiocarbamate; Supramolecular; DNA binding; Anticancer; DNA ladder assay

1. Introduction

Cisplatin and its analogs are the best class of metallo-drugs for the treatment of cancer [1–5]. Despite their effectiveness, there is still room for improvement in terms of reduction in toxicity, increased clinical effectiveness, broader spectrum of action, elimination of side effects (e.g. nausea, hearing loss, and vomiting) and increased solubility. Bioinorganic and medicinal chemists followed two strategies to gain the aforementioned objectives; tuning ligand structure and stereochemistry around the platinum center in order to improve the mode of action and metabolism of these drugs and to use them in combination with other drugs, limited by severe toxicities so far [6].

Palladium derivatives have been explored as an alternative [7] to platinum-based compounds due to their obvious structural and thermodynamic similarities. However, palladium (II) compounds have a rapid rate of hydrolysis leading to reactive species and are thus unable to reach their pharmacological targets. In addition, they are transformed into inactive *trans*-derivatives. The stabilization of Pd(II) compounds by strongly coordinating ligands and suitable leaving group has been exploited as a synthetic strategy to obtain better palladium-based antitumor agents [8]. One of the early studies by Graham and co-workers [9] advocated the use of palladium complexes due to their superior activity to platinum counterparts e.g. cisplatin and carboplatin [10]. The Pd(II) complexes in which palladium is bonded to inert ligands (e.g. sulfur or nitrogen) were suggested by Das and Livingstone [11] to be more effective antitumor agents due to their appropriate labile nature for carrying them to the target DNA. Research groups recently focused on DNA-binding properties of dithiocarbamate-based complexes [12–14] with promising results [15–20]. Furthermore, this class of ligands has attracted attention due to its highly selective role in protecting a variety of animal species from renal, gastrointestinal, and bone marrow toxicity, induced by cisplatin without undermining cisplatin's antitumor effect [21–24]. To further explore non-platinum antitumor drugs, herein, we report two heteroleptic Pd(II) dithiocarbamates with high activity against HeLa cell in comparison with cisplatin.

2. Experimental

2.1. *Materials and methods*

Reagents palladium(II) chloride, 3-methoxyphenylpiperazine, tris(4-chlorophenyl)phosphine, and tris(4-fluorophenyl)phosphine were obtained from Wako Japan. All solvents were purchased from Daejung, Sigma-Aldrich, and Scharlau. Acetic acid, ethylenediaminetetraacetic acid, disodium salt dihydrate (Na_2EDTA), L-glutamine, penicillin-G, pyruvic acid, sodium chloride, sodium dodecyl sulfate (SDS), sodium sarcosinate, streptomycin sulfate, thiazolyl blue tetrazolium bromide (MTT), Triton X-100, and trizma-Base were purchased from Sigma-Aldrich (USA), whereas Dulbecco's Modified Eagle Medium (DMEM) and fetal bovine serum (FBS) were purchased from GibcoBRL, Gaithersburg, MD. The melting points were determined in a capillary tube using a Gallenkamp (UK) electrothermal melting point apparatus. IR spectra from 4000–200 cm^{-1} were obtained on a Thermo Nicolet-6700 FT-IR spectrophotometer. Elemental analysis was done using a CE-440 Elemental Analyzer (Exeter Analytical, Inc.). ^1H and ^{13}C NMR spectra were recorded on a Bruker instrument using TMS as an internal reference. Chemical shifts are given in ppm and coupling constants (J) in Hz. For ^{31}P NMR, 85% H_3PO_4 in water was used as reference.

2.2. *Synthesis*

2.2.1. Synthesis of 1. To 20 mL methanolic suspension of palladium(II) chloride (0.177 g, 1 mmol) in a round bottom three-neck flask was added tris(4-fluorophenyl)phosphine (0.316 g, 1 mmol) solution in acetone (20 mL) and sodium 4-(3-methoxyphenyl)piperazine-1-carbodithioate (0.290 g, 1 mmol) solution in methanol (30 mL) in a dropwise manner. The reaction mixture was refluxed for 6 h with constant stirring. The formed greenish

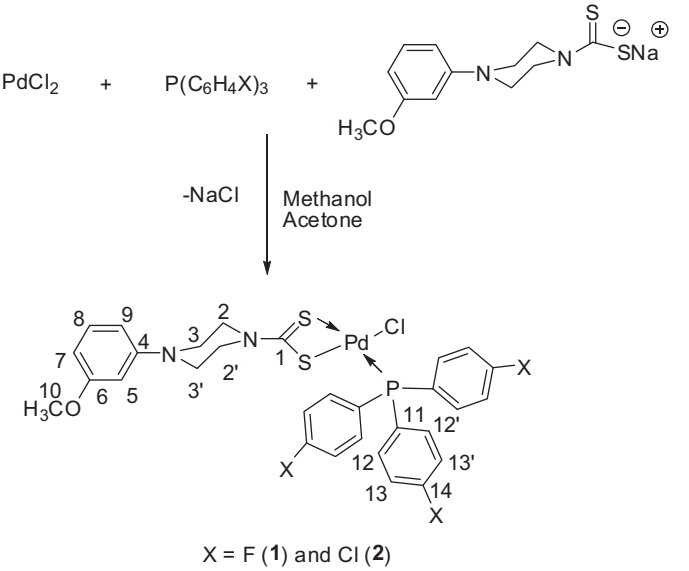

Scheme 1. Synthesis of complexes **1** and **2** along with numbering scheme.

precipitate was separated by filtration (scheme 1). This precipitate was re-dissolved in acetone, and on slow evaporation, needle crystals were obtained.

Yield: (0.470 g, 60%), m.p. 250 °C. Mol. Wt: 745.48: Anal. Calcd $C_{30}H_{27}ClF_3N_2OPPdS_2$: C, 49.62 (49.65); H, 3.72 (3.68); N, 3.86 (3.80); S, 8.82 (8.79): IR (4000–200 cm^{-1}): 1584 ν(C–N); 1002 $\nu(CSS_{sym})$; 250 ν(Pd–S); 338 ν(Pd–Cl); 218 ν(Pd–P): ^{1}H NMR ($CDCl_3$,300 MHz) δ (ppm): 3.81 (s, 3H, H_{10}), 3.89 (t, 4H, H_3, $H_{3'}$, $^3J^1_{H,\ ^1H}$ = 4.8 Hz), 4.06 (t, 4H, H_2, $H_{2'}$, $^3J^1_{H,\ ^1H}$ = 5.1 Hz), 6.44 (s, 1H, H_5), 6.45 (d, 1H, H_9, $^3J^1_{H,\ ^1H}$ = 2.4 Hz), 6.52 (dd, 1H, H_8, $^3J^1_{H,\ ^1H}$ = 2.4, 2.7 Hz), 6.54 (d, 1H, H_7, $^3J^1_{H,\ ^1H}$ = 2.4 Hz), 7.14–7.73 (m, 12H, H_{12}, $H_{12'}$, H_{13}, $H_{13'}$). ^{13}C NMR ($CDCl_3$,75 MHz) δ (ppm): 46.5 (C3, C3′), 48.9 (C2, C2′), 55.3 (C10), 103.6 (C5), 105.9 (C7), 109.6 (C9), 116.0 (C12), 125.3 (C13), 130.2 (C8), 151.4 (C4), 160.7 (C6), 163.2 (C11), 165.7 (C14), 206.2 (C1). ^{31}P NMR (121.49 MHz, $CDCl_3$) δ (ppm): 24.36.

2.2.2. Synthesis of 2. Complex **2** has been synthesized via a synthetic procedure similar to that described for **1** using 0.177 g (1 mmol), 0.365 g (1 mmol) and 0.290 g (1 mmol) palladium(II) chloride, tris(4-chlorophenyl)phosphine and 4-(3-methoxyphenyl)piperazine-1-carbodithioate, respectively. Yield: (0.60 g, 72%) m.p. 206 °C: Mol. Wt: 774.82: Anal. Calcd for $C_{30}H_{27}Cl_4N_2OPPdS_2$: C, 46.46 (46.50); H, 3.48 (3.58); N, 3.61 (3.65); S, 8.26 (8.30): IR (4000–200 cm^{-1}): 1598 ν(C–N), 996 $\nu(CSS_{sym})$, 248 ν(Pd–S), 344 ν(Pd–Cl); 227 υ(Pd–P): ^{1}H NMR ($CDCl_3$,300 MHz) δ (ppm): 3.81 (s, 3H, H_{10}), 3.87 (t, 4H, H_3, $H_{3'}$, $^3J^1_{H,\ ^1H}$ = 4.8 Hz), 4.05 (t, 4H, H_2, $H_{2'}$, $^3J^1_{H,\ ^1H}$ = 5.1 Hz), 6.46 (s, 1H, H_5), 6.51 (d, 1H, H_7, $^3J^1_{H,\ ^1H}$ = 3.0 Hz), 6.52 (dd, 1H, H_8, $^3J^1_{H,\ ^1H}$ = 2.4, 2.7), 6.55 (d, 1H, H_9, $^3J^1_{H,\ ^1H}$ = 2.7 Hz), 7.19–7.64 (m, 12H, H_{12}, $H_{12'}$, H_{13}, $H_{13'}$). ^{13}C NMR ($CDCl_3$,75 MHz) δ (ppm): 49.0 (C3, C3′), 55.3 (C10), 53.8 (C2, C2′), 103.6 (C5), 105.9 (C7), 109.6 (C9), 129.1 (C13), 130.2 (C8), 135.9 (C14), 136.1 (C12), 137.9 (C11), 151.4 (C4), 160.7 (C6), 206.0 (C1). ^{31}P NMR (121.49 MHz, $CDCl_3$) δ (ppm): 24.95.

2.3. *X-ray single-crystal analysis*

The X-ray single-crystal analysis of **1** and **2** was carried out on a Bruker Kappa APEX-II CCD diffractometer having a CCD detector set 40.0 mm from the crystals. From a sealed ceramic diffraction tube (SIEMENS) having graphite monochromated Mo-Kα radiation, different intensities were determined. Then, using Patterson and DIRDIF method, the structure of the compound was solved. Further refinement on F^2 was carried out by full-matrix least squares using SHELXL-97 [25]. The details are given in tables 1 and 2.

2.4. *DNA interaction study by UV–vis spectroscopy*

Calf thymus DNA (CT-DNA) (20 mg) was dissolved in double deionized water (pH 7.0) and kept at 4 °C for less than 4 days. The nucleotide to protein (N/P) ratio of ~1.9 was obtained from the ratio of absorbance at 260 and 280 nm (A260/A280 = 1.9), indicating that the DNA was sufficiently free from protein [26]. The concentration of CT-DNA was determined spectrophotometrically using the molar absorption coefficient 6600 M^{-1} cm^{-1} (260 nm) [27] and was found to be 3.1×10^{-4} M. Then, from this stock solution 5, 10, 15, 20 and 25 μM, working solutions were prepared by dilution method. The 37.6 μM of **1** and 22.96 μM of **2** were prepared in 98% DMSO. The UV absorption titrations were performed by keeping the

Table 1. Crystal data and refinement parameters of **1** and **2**.

Crystal data	**1**	**2**
Chemical formula	$C_{30}H_{27}ClF_3N_2OPPdS_2$	$C_{30}H_{27}Cl_4N_2OPPdS_2$
Formula weight (g mol^{-1})	725.48	774.82
Crystal system	Monoclinic	Monoclinic
Space group	$P2_1/c$	$P2_1/c$
T (K)	296(2)	296(2)
Wavelength (Å)	0.71073	0.71073
Cell parameters		
a (Å)	19.5880(10)	20.221(8)
b (Å)	10.1763(5)	10.285(4)
c (Å)	16.4172(7)	17.469(6)
α (°)	90.00	90
β (°)	106.920(2)	113.683(14)
γ (°)	90.00	90
V (Å^3)	3130.8(3)	3327(2)
Z	4	4
Absorption coefficient (mm^{-1})	0.907	1.080
F(0 0 0)	1464.0	1560.0
Data collection		
2Θ range for data collection (°)	4.34–56.42	4.4–55.95
Number of collected reflections	26,754	29,848
Number of independent reflections	7569	7921
Goodness of fit on F^2	0.969	1.001
Final R indexes [$I \geq 2\sigma(I)$]	$R_1 = 0.0359$, $wR_2 = 0.0711$	$R_1 = 0.0486$, $wR_2 = 0.0893$
Final R indexes [all data]	$R_1 = 0.0752$, $wR_2 = 0.0848$	$R_1 = 0.1072$, $wR_2 = 0.1079$

Table 2. Selected bond lengths and angles for **1** and **2**.

	Bond length (Å)			Bond angle (°)	
Type of bond	**1**	**2**	Type of bond	**1**	**2**
Pd1–Cl1	2.3266(8)	2.3312(13)	P1–Pd1–S2	95.99(3)	170.59(4)
Pd1–S1	2.3473(8)	2.2836(13)	P1–Pd1–Cl1	92.30(3)	91.17(4)
Pd1–S2	2.2770(8)	2.3435(14)	S2–Pd1–Cl1	171.16(3)	97.45(5)
Pd1–P1	2.2672(8)	2.2558(14)	P1–Pd1–S1	168.46(3)	96.17(4)
C1–S1	1.715(3)	1.723(4)	S2–Pd1–S1	75.57(3)	75.42(4)
C1–S2	1.722(3)	1.721(4)	Cl1–Pd1–S1	96.63(3)	172.20(4)
C1–N1	1.314(3)	1.302(5)			

concentration of the compound fixed while varying the DNA concentration. During the titration DNA solution (5–25 μM) was added to each cuvette (1 cm path length) to eliminate the absorbance of DNA itself, and the solutions were mixed by repeated inversion. After the solutions were mixed for ~5 min, the absorption spectra were recorded at room temperature from 200 to 800 nm. The titration processes were repeated until there was no change in the spectra for four titrations at least, indicating binding saturation had been achieved.

2.5. In vitro *studies: cell culture and cytotoxicity analysis on HeLa*

Human cervix adenocarcinoma (HeLa, ATCC CCl-2) cells were maintained in DMEM containing FBS (10%), Na-pyruvate (1 mM), L-glutamine (2 mM), penicillin (100 U mL^{-1}), and streptomycin (100 μg mL^{-1}) under a humidified atmosphere at 5% CO_2 and 37 °C.

The cytotoxicity of the compounds was measured by MTT assay as described earlier [28]. In short, HeLa cultures (>90% viability; 1.5×10^5 cells mL^{-1}) were exposed to six different concentrations (1, 3, 10, 30, 100, and 300 μM) of the two compounds and cisplatin for 24 h.

As experimental controls, unexposed samples, DMSO (solvent) treated and non-cellular background samples, i.e., "media only" and "compound only" were included in each experiment. Then, cultures were incubated with MTT solution (0.5 mg mL^{-1}) for 3 h at 37 °C to produce formazan crystals which were dissolved in acidified 10% SDS, and absorbance was measured at 565 nm using a microplate reader (AMP PLATOS R-496). Relative percent viability of the treated samples was calculated using the following formula:

$$\text{Relative percent viability} = [\text{Abs}\,(565)_{\text{test}} - \text{Abs}\,(565)_{\text{compound control}}/\text{Abs}\,(565)_{\text{unexposed control}} - \text{Abs}\,(565)_{\text{media}}] \times 100,$$

where Abs $(565)_{\text{test}}$ and Abs $(565)_{\text{unexposed control}}$ represent the optical density at 565 nm for the treated samples and untreated control samples, respectively. Abs $(565)_{\text{compound control}}$ and Abs $(565)_{\text{media}}$ represent background optical density and was measured in compound only and media only samples, respectively. The IC_{50} value for the compounds (the experiment was performed twice with triplicates each) representing the concentrations at which 50% of cell growth is inhibited was calculated.

2.6. *DNA ladder assay for apoptosis*

The DNA fragmentation (DNA ladder) following treatment with the test compounds was assessed by agarose gel electrophoresis according to Enari *et al.* [29] with slight modifications. Briefly, HeLa (>90% viability; 1×10^6) cells were exposed to IC_{50} concentrations of the compounds and cisplatin for 4 h. DMSO treated and untreated control samples were also included in the experiment. Cells were collected and centrifuged at 1200 rpm for 5 min, washed once with PBS and resuspended in a lysis buffer [Tris–HCl (50 mM pH 8.0), ethylenediamine tetraacetic acid (5 mM), SDS (1.2%), NaCl (150 mM), and proteinase K (0.2 mg mL^{-1})] and incubated overnight at 37 °C. DNA was isolated by salting out method and quantified using a NanoDrop 2000 spectrophotometer. Four microgram DNA was loaded into the wells of a 2% agarose gel using cut tips. Electrophoresis was carried out in TBE buffer at 60 V for 2 h, and DNA fragments were visualized by ethidium bromide staining.

2.7. *Statistical analysis*

The data from the biological activity experiments are presented as mean ± standard deviation. ANOVA (One-way) and *t*-test (two tailed) were used to statistically analyze the differences between unexposed, DMSO (solvent) exposed, and compound-treated samples. Results were considered significant at $\alpha = 5\%$.

3. Results and discussion

3.1. *Chemistry*

Complexes **1** and **2** were synthesized in good yield and were soluble in common organic solvents.

3.2. *Spectral characterization*

FT-IR spectroscopy is a powerful tool to assess the nature of bonding and mode of coordination in transition metal dithiocarbamates. The presence of Pd–S stretch at 250 cm^{-1} (**1**) and 248 cm^{-1} (**2**) which was absent in corresponding precursors indicated the coordination of dithiocarbamate to Pd [30]. The Pd–Cl stretch at 338 and 344 cm^{-1} for **1** and **2** signifies the removal of only one chloride from $PdCl_2$ during complexation. The attachment of substituted triphenylphosphine was indicated by the presence of Pd–P stretch at 218 and 227 cm^{-1}. The presence of a single band associated with C–S vibration at 1002 and 996 cm^{-1} in **1** and **2** is in accord with bidentate coordination [31]. The presence of C–N stretch at 1584 cm^{-1} (**1**) and 1598 cm^{-1} (**2**) is an indication of partial double bond character in the C–N bond.

The assignment of the proton resonances was made by their chemical shift value, peak multiplicity, intensity pattern, and comparison of the integration values of the protons with expected composition. The ^{1}H spectra of the ligand, **1,** and **2** were recorded in $CDCl_3$ using tetramethylsilane (TMS) as internal standard. The presence of proton resonances for ligand and organophosphine confirmed the formation of **1** and **2**. The methylene protons of N–$(CH_2)_2$ are a triplet at 3.89–4.06 and 3.87–4.05 ppm in **1** and **2**, respectively, in agreement with the observation made by Manav *et al.* [23]. Methoxy protons were detected at 3.81 ppm as a singlet for **1** and **2**. The phenyl protons are at 6.44–6.54 ppm for both compounds.

The number of signals observed in ^{13}C NMR spectra of **1** and **2** was as expected. No significant change was observed except the CS_2 carbon chemical shift which moved upfield from 214.7 ppm (ligand) to 206.2 ppm (**1**) and 206.0 ppm (**2**). This upfield shift is due to shielding of 1,1-dithioate carbon resulting from mobilization of the nitrogen lone pair upon complexation of the two sulfurs with palladium center. The ^{31}P chemical shifts of **1** and **2** were observed at 24.36 and 24.95 ppm, respectively. The downfield shift of ^{31}P value in Pd (II) complexes from free organophosphines confirms the coordination of phosphorus to palladium.

3.3. *Solid-state structures of 1 and 2*

Crystal data and refinement parameters for **1** and **2** are given in table 1 while selected bond lengths and angles are given in table 2. The crystal system of both compounds is monoclinic with $P2_1/c$ space group. Both compounds show square-planar geometry with dithiocarbamate occupying two adjacent coordination sites of Pd(II) while the chloride and organophosphine occupy the remaining sites. The largest distortion from the normal geometry comes from the bidentate ligand S(1)–Pd(1)–S(2) of 75.57(3)° and S(1)–Pd(1)–S(2) of 75.42(4)° for **1** and **2**, respectively. The asymmetry observed in the Pd–S distance is typical for square-planar systems and is reflecting the *trans* effect of the ligand. Pd(1)–S(1) bond lengths are longer [2.3473(8) Å and 2.2836(13) Å] than Pd(1)–S(2) bond length [2.2770(8) Å and 2.3435(14) Å] with ΔPd–S of 0.0703 Å (**1**) and 0.0599 (**2**). The bond length of C(1)–S(1) [1.715(3) Å and 1.723(4) Å for **1**] and of C(1)–S(2) [1.722(3) Å and 1.721(4) Å for **2**] is in between single bond C–S (1.82 Å) and double bond C=S (1.60 Å) values [32]. Similarly, the C(1)–N(1) bond length is 1.314(3) Å and 1.302(5) Å for **1** and **2**, shorter than the normal C–N bond distance (1.47 Å) and longer than a C=N bond length (1.28 Å) [33], thus signifying a resonance phenomenon in the NSCS moiety.

The crystal packing of **1** revealed 3-D-supramolecular network composed of various 1-D chains mediated by various interactions (figure 1). As shown in figures S1a and S1b (see online supplemental material at http://dx.doi.org/10.1080/00958972.2015.1054817), molecules are arranged in antiparallel fashion in the chains by self-complementary CH···S [C(2)-H(2B)···S(1) 2.915 Å], CH···π [C(27)–H(27)···C(10) 2.881 Å], and CH···Cl [C(8)-H(8)···Cl (1) 2.871 Å] interactions. Each chain of the network is connected to the neighboring chains with the help of CH···F [C(17)–H(17)···F(3) 2.625 Å], CH···Cl–Pd [C(2)–H(2A)···Cl(1) 2. 949 Å], CH···π [C(5)–H(5B)···C(10) 2.773 Å], and halide-π [F(1)···C(23) 3.085 Å] interactions. The adjacent 1-D chains extend into a 3-D supramolecular network by self-complementary CH···F [C(21)–H(21)···F(1) 2.505 Å] interactions [figures S2(a-d)].

In **2,** the same interactions were observed as for **1**, however, with slightly different distances (figure 2). Interestingly, the change of substituents at triphenylphosphine moiety of **2** led to formation of similar 3-D-supramolecular network comprised of various 1-D chains as in **1**, despite having different non-covalent interactions. As shown in figures S2a and S2b, molecules are arranged in antiparallel fashion in the individual chains of the network by self-complementary CH···S [C(2)–H(2B)···S(2) 2.931 Å], CH···π [C(21)–H(21)···C(10) 2.826 Å], and CH···Cl [C(18)–H(18)···Cl(4) 2.938 Å] interactions. Each chain of the network is further connected to neighboring chains with CH···O [C(5)–H(5B)···O(1) 2.636 Å], CH···π [C(5)-H(5B)···C(10) 2.861 Å], and halide-π [Cl(2)···C(29) 3.389 Å, Cl(3)···C(27) 3.432 Å] interactions. Adjacent 1-D chains extend into a 3-D supramolecular network by CH···π [C(27)–H(27)···C(17) 2.732 Å] interactions (figures S2a–d). Surprisingly, the CH···O interactions present in **2** were not observed in **1**, however, an additional Pt–Cl···H interaction was found in the latter.

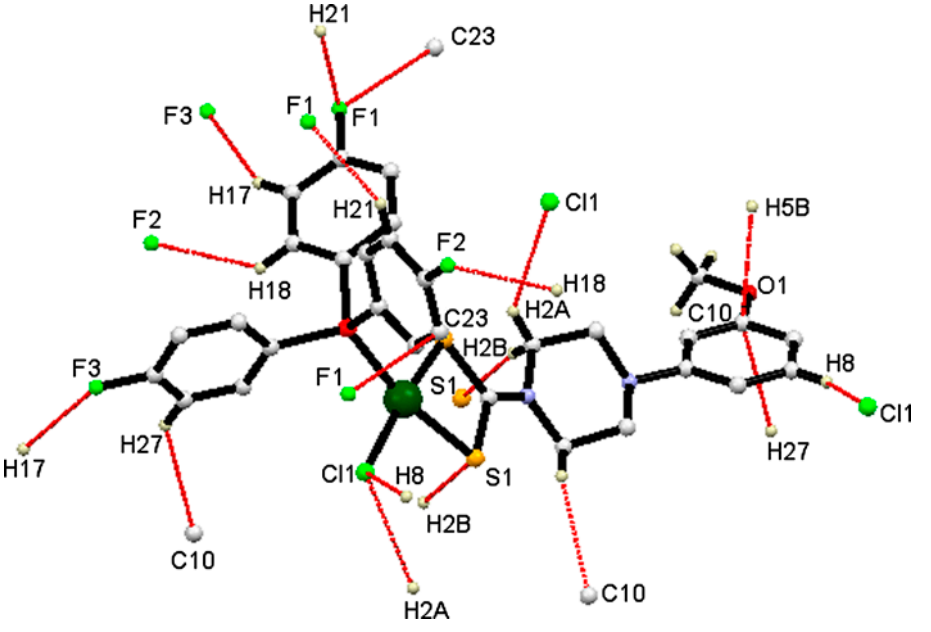

Figure 1. Contribution of phosphine and dithiocarbamate to supramolecular assemblies.
Note: Hydrogen not involved in non-covalent interactions are omitted for clarity.

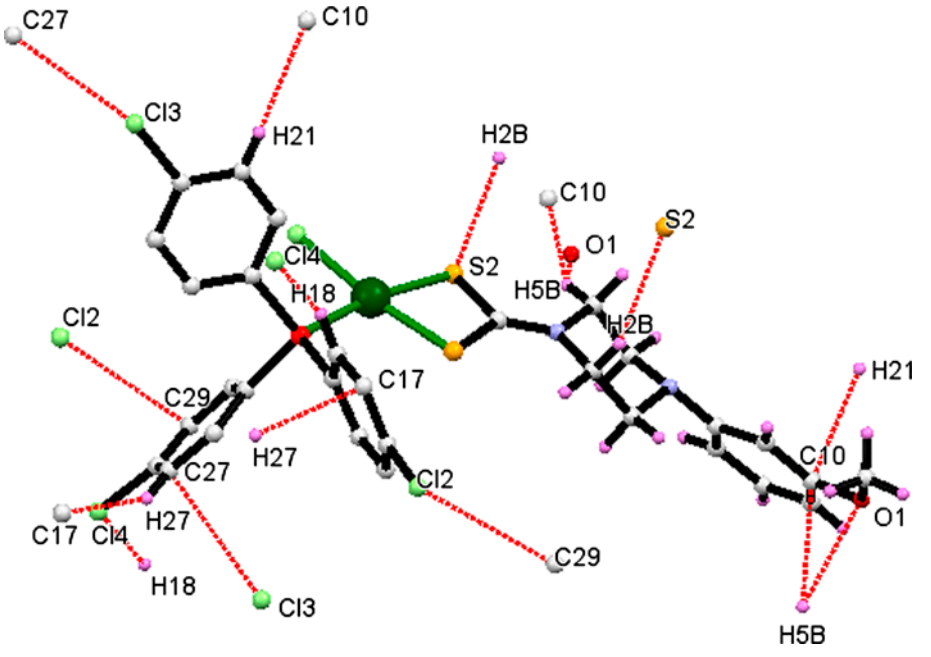

Figure 2. Contribution of phosphine and dithiocarbamate to supramolecular assemblies of **2**.
Note: Hydrogen not involved in non-covalent interactions are omitted for clarity.

3.4. *DNA-binding studies*

UV–vis spectroscopy is a powerful tool to assess drug–DNA binding studies [34]. A complex binding to DNA through intercalation usually results in hypochromism and bathochromism. In this mode of binding to DNA, the π^* orbital of the binding ligand could couple with the π orbital of base pairs in DNA. The coupling π^* orbital is partially filled by electrons, thus decreasing the transition probabilities, and hence resulting in the hypochromicity [35]. The extent of the hypochromism commonly parallels the intercalative binding affinity [36]. For **1** and **2**, a gradual reduction in peak intensity by titrating fixed complex concentration with increasing DNA accompanied by a slight red shift of ~2 nm (figures 3 and 4) signifies intercalative interaction [37].

Based upon the variation in absorbance, the association/binding constants of these complexes with DNA were determined according to the Benesi–Hildebrand equation, equation (1) [38]:

$$\frac{A_0}{A - A_0} = \frac{\varepsilon_G}{\varepsilon_{H-G} - \varepsilon_G} + \frac{\varepsilon_G}{\varepsilon_{H-G} - \varepsilon_G} \times \frac{1}{K[\mathrm{DNA}]} \quad (1)$$

where K is the association/binding constant, A_0 and A are the absorbance of the compound and its complex with DNA, respectively, and ε_G and ε_{H-G} are the absorption coefficients of the compound and the compound-DNA complex, respectively. The association constants obtained were $2.402 \times 10^4\ M^{-1}$ (**1**) and $2.713 \times 10^3\ M^{-1}$ (**2**) from the intercept-to-slope ratios of $A_0/(A - A_0)$ *versus* 1/[DNA] plots. The Gibb's free energy (ΔG) was determined from equation (2):

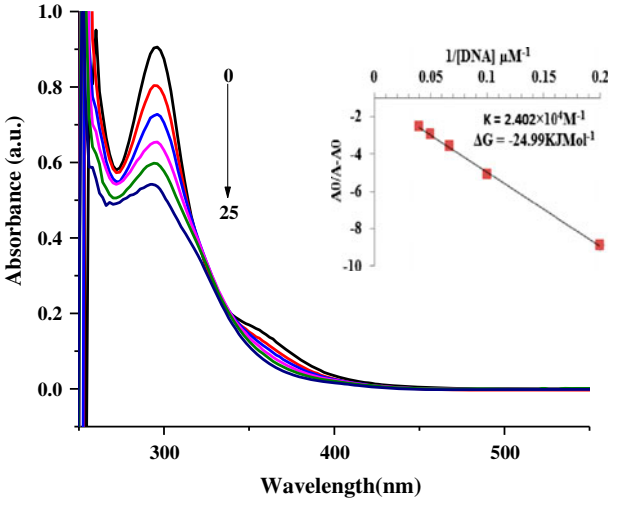

Figure 3. Absorption spectrum of 37.6 μM **1** in the absence (a) and presence of (b) 5, (c) 10, (d) 15, (e) 20, (f) 25, μM DNA.
Note: The inset graph represents the plot of $A_0/A - A_0$ *vs.* 1/[DNA] $(\mu M)^{-1}$ for calculation of binding constant (K) and Gibb's free energy (ΔG).

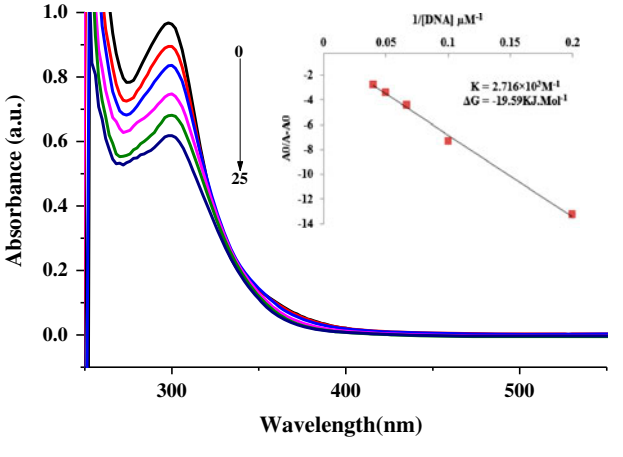

Figure 4. Absorption spectrum of 22.96 μM **2** in the absence (a) and presence of (b) 5, (c) 10, (d) 15, (e) 20, (f) 25, μM DNA.
Note: The inset graph represents the plot of $A_0/A - A_0$ *vs.* 1/[DNA] $(\mu M)^{-1}$ for calculation of binding constant (K) and Gibb's free energy (ΔG).

$$\Delta G = -RT \ln K \tag{2}$$

where R is the general gas constant (8.314 JK^{-1} mol^{-1}) and T is the temperature (298 K) and was calculated to be −24.99 kJ mol^{-1} (**1**) and −19.59 kJ mol^{-1} (**2**), thus indicating that drug–DNA binding is spontaneous.

3.5. In vitro *studies: cytotoxicity analysis on HeLa*

Complexes **1**, **2,** and cisplatin were screened for their anticancer activity against the HeLa cell line at six different concentrations (1, 3, 10, 30, 100, and 300 μM). As shown in figure S3, **1** and **2** showed strong cytotoxic activity against the cells when compared to cisplatin. The IC_{50} values (table 3) of **1** and **2** were 22 ± 3 and 26 ± 3 μM, respectively, whereas Cisplatin had an IC_{50} of 78 ± 4 μM which signify that the complexes were almost four times more active than Cisplatin. The anticancer activities of **1** and **2** are largest of the reported palladium complexes with ligands other than dithiocarbamate [39].

3.6. *DNA ladder assay for apoptosis*

As the two complexes showed good DNA interaction in the DNA-binding studies and were toxic to HeLa cells, these were further tested for their ability to induce DNA fragmentation *in vitro* using a DNA ladder assay. As shown in figure 5, both **1** and **2** caused strong DNA fragmentation as compared to Cisplatin. These observations are consistent with results obtained from drug DNA interaction studies and cytotoxicity analysis on the HeLa cell line. Our findings suggest that the cytotoxicity of these compounds might be due to strong interaction with DNA leading to DNA damage and apoptosis. Induction of DNA damage to manage cancer cells is an old and very attractive tool [40, 41]. The complexes exhibit much higher activity than Cisplatin. Achieving stronger effects at low doses will help with the

Table 3. Anticancer activities of **1**, **2,** and Cisplatin.

Cell line	Complexes	IC_{50} (μM)
Hela	**1**	22 ± 3
	2	26 ± 3
	Cisplatin	78 ± 4

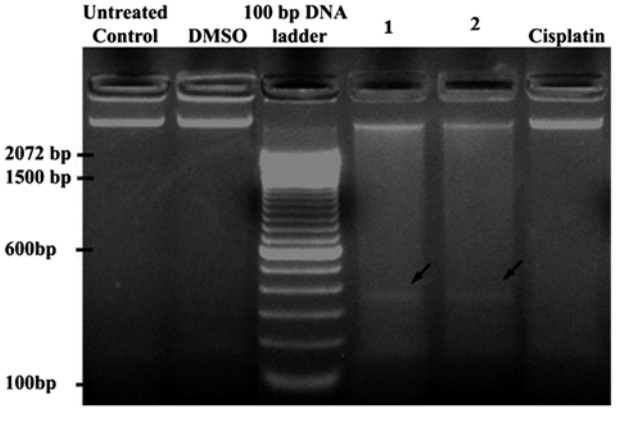

Figure 5. DNA fragmentation following treatment of the compounds and Cisplatin. HeLa cells were treated with IC_{50} concentration of **1** and **2** for 3 h. Their DNA was extracted, and 4 μg DNA was electrophoresed on 1.5% Agarose gel.

problem of drug resistance as observed for Cisplatin [40, 42]. Understanding the biology effects, cellular mechanisms involved and response of the DNA repair pathways may also give benefit in the clinics [43, 44].

4. Conclusion

We have synthesized two new heteroleptic Pd(II) dithiocarbamates (**1** and **2**) and characterized them on the basis of their physical, spectral (IR, ^{1}H and ^{13}C NMR), and X-ray crystallographic data. Square-planar geometry of both complexes is observed in solution as well as in the solid state. Although both complexes showed similar packing (3-D-supramolecular networks) in the solid state, the nature and strength of various non-covalent interactions involved in the stabilization of these networks are different. Stronger and greater number of interactions were observed in **1** (18 interactions per molecule) than **2** (16 interactions per molecule). For example, the CH···O interactions observed in **2** are absent in **1**, similarly Pt–Cl···H interactions are observed in the latter only. This shows that small changes may lead to a cascade of changes in non-covalent interactions. The DNA interaction studies by UV–visible spectroscopy showed that the complex with better and stronger capability of non-covalent interaction is a better DNA binder, $2.402 \times 10^{4}\ M^{-1}$ (**1**) and $2.713 \times 10^{3}\ M^{-1}$ (**2**). The same trend was reflected in anticancer activity where **1** ($IC_{50} = 22\ \mu M$) and **2** (26 μM) were more active than Cisplatin (78.075 μM). So there seems to be a connection between non-covalent interactions, DNA binding, and anticancer activity. In addition, DNA fragmentation suggested that the anticancer action of these complexes stems from their interaction with DNA leading to DNA damage and apoptosis. The outstanding anticancer results of **1** and **2** demand further *in vivo* investigations.

Supplementary material

Single-crystal X-ray diffraction data for the structural analysis have been deposited with the Cambridge Crystallographic Data Center, CCDC Nos. 1038602 (**1**) and 1038603 (**2**). A copy of this information may be obtained free of charge from the Director, CCDC, 12 Union Road, Cambridge, CBZ 1EZ, UK (Fax: +44 1223 336033; Email: deposit@ccdc.cam.ac.uk or www: http://www.ccdc.cam.ac.uk).

Acknowledgements

We acknowledge the financial support from TWAS (Third World Academy of Science) and Higher education Commission of Pakistan.

Disclosure statement

No potential conflict of interest was reported by the authors.

References

[1] M. Shaharyar, M.M. Abdullah, M.A. Bakht, J. Majeed. *Eur. J. Med. Chem.*, **45**, 114 (2010).
[2] T. Boulikas, M. Vougiouka. *Oncol. Rep.*, **10**, 1663 (2003).
[3] E. Wong, C.M. Giandomenico. *Chem. Rev.*, **99**, 2451 (1999).
[4] M. Galanski, V.B. Arion, M.A. Jakupec, B.K. Keppler. *Curr. Pharm. Des.*, **9**, 2078 (2003).
[5] D. Wang, S.J. Lippard. *Nat. Rev. Drug Discov.*, **4**, 307 (2005).
[6] A.S. Abu-Surrah, H.H. Al-Sa'doni, M.Y. Abdalla. *Cancer Ther.*, **6**, 1 (2008).
[7] A.C.F. Caires. *Anti-Cancer Agents Med. Chem.*, **7**, 484 (2007).
[8] A.S. Abu-Surrah, M. Kettunen. *Curr. Med. Chem.*, **13**, 1337 (2006).
[9] R.D. Graham, D.R. Williams. *J. Inorg. Nucl. Chem.*, **41**, 1245 (1979).
[10] A.R. Kapdi, I.J.S. Fairlamb. *Chem. Soc. Rev.*, **43**, 4751 (2014).
[11] M. Das, S.E. Livingstone. *Br. J. Cancer*, **37**, 466 (1978).
[12] H. Mansouri-Torshizi, M. Islami-Moghaddam, A. Divsalar, A.A. Saboury. *Bioorg. Med. Chem.*, **16**, 9616 (2008).
[13] M. Islami-Moghaddam, H. Mansouri-Torshizi, A. Divsalar, A.A. Saboury. *J. Iran. Chem. Soc.*, **6**, 552 (2009).
[14] (a) H. Khan, A. Badshah, M. Said, G. Murtaza, J. Ahmad, B.J. Jean-Claude, M. Todorova, I.S. Butler. *Appl. Organomet. Chem.*, **27**, 387 (2013); (b) H. Khan, Zia-ur-Rehman, A. Shah, M. Said, G. Murtaza, I.S. Butler, S. Ahmed, F.G. Fontaine, A. Badshah. *Polyhedron*, **39**, 1 (2012); (c) H. Mansouri-Torshizi, M.I. Moghaddam, A. Divsalar, A.A. Saboury. *J. Biomol. Struct. Dyn.*, **26**, 575 (2009).
[15] M. Saeidfar, H. Masouri-Torshizi, G.R. Behbehani, A.A. Saboury, A. Divsalar. *Bull. Korean Chem. Soc.*, **30**, 1951 (2009).
[16] L. Ronconi, C. Maccato, D. Barreca, R. Saini, M. Zancato, D. Fregona. *Polyhedron*, **24**, 521 (2005).
[17] L. Ronconi, L. Giovagnini, C. Marzano. *Inorg. Chem.*, **44**, 1867 (2005).
[18] K. Unoura, A. Yamazaki, A. Nagasawa. *Inorg. Chim. Acta*, **269**, 260 (1998).
[19] H. Teruel, Y.C. Gorrín, L.R. Falvello. *Inorg. Chim. Acta*, **316**, 1 (2001).
[20] H. Zheng, W.H. Leung, J.L.C. Chim. *Inorg. Chim. Acta*, **306**, 184 (2000).
[21] M.A. Zemaitis, F.E. Greene. *Toxicol. Appl. Pharmacol.*, **48**, 343 (1979).
[22] R. Mital, N. Jain, T.S. Srivastava. *Inorg. Chim. Acta*, **166**, 135 (1989).
[23] N. Manav, A.K. Mishra, N.K. Kaushik. *Spectrochim. Acta, Part A*, **65**, 32 (2006).
[24] G. Faraglia, S. Sitran, D. Montagner. *Inorg. Chim. Acta*, **358**, 971 (2005).
[25] G.M. Sheldrick. *Acta Crystallogr. A*, **64**, 112 (2008).
[26] O. Warburg, W.Z. Christian. *Biochemistry*, **310**, 384 (1942).
[27] M.E. Reichmann, S.A. Rice, C.A. Thomas, P. Doty. *J. Am. Chem. Soc.*, **76**, 3047 (1954).
[28] T. Mosmann. *J. Immunol. Methods*, **65**, 55 (1983).
[29] M. Enari, H. Sakahira, H. Yokoyama, K. Okawa, A. Iwamatsu, S. Nagata. *Nature*, **391**, 43 (1998).
[30] E.D. Risberg, J. Mink, A. Abbasi, M.Yu. Skripkin, L. Hajba, P. Lindqvist-Reis, E. Bencze, M. Sandstrom. *Dalton Trans.*, 1328 (2009).
[31] F. Shaheen, A. Badshah, M. Gielen, G. Croce, U. Florke, D.D. Vos, S. Ali. *J. Organomet. Chem.*, **695**, 315 (2010).
[32] H. Khan, A. Badshah, G. Murtaz, M. Said, Rehman, C. Neuhausen, M. Todorova, B. J. Jean-Claude, I.S. Butler. *Eur. J. Med. Chem.*, **46**, 4071 (2011).
[33] F.H. Allen, O. Kennard, D.G. Watson, L. Brammer, A.G. Orpen, R. Taylor. *J. Chem. Soc., Perkin Trans.*, **2**, S1, (1987).
[34] J.K. Barton, A. Danishefsky, J. Goldberg. *J. Am. Chem. Soc.*, **106**, 2172 (1984).
[35] C.C. Ju, A.G. Zhang, C.L. Yuan, X.L. Zhao, K.Z. Wang. *J. Inorg. Biochem.*, **105**, 435 (2011).
[36] S. Shi, J. Liu, J. Li, K.-C. Zheng, X.-M. Huang, C.-P. Tan, L.-M. Chen, L.-N. Ji. *J. Inorg. Biochem.*, **100**, 385 (2006).
[37] G. Yunus, S. Srivastava, V.D. Gupta. *Int. J. Biophy.*, **2**, 7 (2012).
[38] S. Shujha, A. Shah, Zia-ur-Rehman, N. Muhammad, S. Ali, R. Qureshi, N. Khalid, A. Meetsma. *Eur. J. Med. Chem.*, **45**, 2902 (2010).
[39] X. Hou, X. Li, H. Hemit, H.A. Aisa. *J. Coord. Chem.*, **67**, 461 (2014).
[40] K. Cheung-Ong, G. Giaever, C. Nislow. *Chem. Biol.*, **20**, 648 (2013).
[41] D. Michod, C. Widmann. *Crit. Rev. Oncol. Hematol.*, **63**, 160 (2007).
[42] R. Drost, J. Jonkers. *Oncogene*, **33**, 3753 (2014).
[43] K. Gurova. *Future Oncol.*, **5**, 1685 (2009).
[44] R. Plummer. *Clin. Cancer Res.*, **16**, 4527 (2010).